

Analysis of radiation-induced
analgesia-related proteins
in an animal model of cancer pain.

Hee Chul Park

Department of Medicine

The Graduate School, Yonsei University

Analysis of radiation-induced
analgesia-related proteins
in an animal model of cancer pain.

Directed by Professor Jinsil Seong

The Doctoral Dissertation
submitted to the Department of Medicine,
the Graduate School of Yonsei University
in partial fulfillment of the requirements
for the degree of Doctor of Philosophy

Hee Chul Park

June 2004

This certifies that
the Doctoral Dissertation
of Hee-Chul Park is approved.

Jinsil Seong, MD. PhD.

Kwang Hoon Lee, MD. PhD.

Kyung-Ah Park, MD. PhD.

Bae Hwan Lee, PhD.

Je-Kyeong Sung, PhD.

The Graduate School
Yonsei University

June 2004

ACKNOWLEDGEMENTS

I am indebted and most appreciative of the efforts of Jeung Hee An, PhD, Jiyoung Kim, MS, Wonwoo Kim, BS, whose expertise and timeliness in making this experiment a success.

I wish to thank Professor Jinsil Seong, the director of this doctoral dissertation. She also directed the course of masters degree of mine. The special thanks goes for her kindness in guiding me a right way in my research. I was always happy with her leadership.

The very special thanks goes to all the referees, Professor Kwang Hoon Lee, Professor Kyung-Ah Park, Professor Bae Hwan Lee, Professor Je-Kyeong Sung.

Particular thanks are given to Professor Hoonsik Bae, Professor Byung Chul Cho, the colleagues in the department of radiation oncology, Hallym University Medical College, for their trouble and careful consideration.

Thanks are also due to my family, Kye Jung, Namu, Sandeul, Father, Mother, Parents in law, who endured my efforts in the preparation of this dissertation.

Finally, I shall be eternally grateful to my teachers, Professor Gwi Eon Kim, Professor Chang Ok Suh. They take a quite fatherly interest in me, always. I am indebtedness to them for the accomplishments I hold now.

June, 2004
Hee Chul Park

TABLE OF CONTENTS

ABSTRACT	1
I. INTRODUCTION	3
II. MATERIALS AND METHODS	4
1. Animal model	4
2. The detection of the invasion of cancer cells to the bone	5
3. The analysis of the behavioral responses to evoked pain stimulations	5
4. Radiotherapy	6
5. Two-dimensional SDS gel electrophoresis (2-DE) and image analysis	6
6. Protein identification by matrix-assisted laser desorption ionization time-of-flight mass spectrometry (MALDI-TOF MS)	7
7. Western blot analysis	8
8. Immunohistochemical staining	9
9. The statistical analysis	9
III. RESULTS	10
1. The establishment of an animal model	10
A. The detection of the invasion of cancer cells to the bone ----	10
B. Behavioral evidences of the development of bone pain resulting from the invasion of cancer cells to the bone	10
2. Radiation-induced relief of bone pain resulting from the invasion of cancer cells to the bone	14

3. Two-dimensional SDS gel electrophoresis (2-DE) and matrix-assisted laser desorption ionization time-of-flight mass spectrometry (MALDI-TOF MS) -----	14
A. Proteins identified in the spinal cord -----	14
B. The differential expression of protein in the spinal cord -----	17
C. Radiation-induced analgesia-related proteins in the spinal cord -----	17
4. Validation of the proteins -----	28
A. Validation of P2X purinoreceptor 6 by Western blot analysis -----	28
5. The effector neurotransmitter mediated by cytosolic Ca ²⁺ and Ca ²⁺ /calmodulin-dependent protein kinase type 1 -----	28
IV. DISCUSSION -----	35
V. CONCLUSION -----	40
REFERENCES -----	41
ABSTRACT (IN KOREAN) -----	46

LIST OF FIGURES

Figure 1. The development of the hind paw model of bony pain due to invasion of cancer cells in the bone -----	11
Figure 2. The relief of pain in the hind paw model of bony pain by radiotherapy -----	15
Figure 3. A reference 2-DE map of spinal cord protein of normal mice (group N) -----	18
Figure 4. Coomassie brilliant blue G250 stained 2-D gels of spinal cord proteins of normal mice (N), tumor-bearing mice (T), and tumor-bearing mice treated with radiation (TR), respectively -----	29
Figure 5. Identification of secretagoin, syntenin, P2X purinoreceptor 6 and CaM kinase 1 by MALDI-TOF mass spectrometry -----	32
Figure 6. Western blot analysis of spinal cord proteins for P2X purinoreceptor 6 and α -tubulin in normal mice (N), tumor-bearing mice (T), and tumor-bearing mice treated with radiation (TR), respectively -----	32
Figure 7. The changes of the pain-related signals in the spinal cord -----	34

LIST OF TABLES

- Table 1. Proteins of mice spinal cord identified by
MALDI-TOF mass spectrometry for the 2-D gel
(pI 3.0 to 10.0) shown in Figure 1 ----- 19
- Table 2. The altered expression of spinal cord proteins by
tumor formation in the ipsilateral hind paw of
normal mice and by radiation to the tumor-bearing
mice and normal mice ----- 23
- Table 3. The proteins in which the increased expression
caused by tumor formation was reversed by
radiation on tumor-bearing mice ----- 27

ABSTRACT

Analysis of radiation-induced analgesia-related proteins
in an animal model of cancer pain

Hee Chul Park

Department of Medicine
The Graduate School, Yonsei University

(Directed by Professor Jinsil Seong)

To explore the mechanism of radiation-induced analgesia, we have developed the model of bone pain resulting from the invasion of cancer cells in C3H/HeJ mice. Using that animal model, the radiation-induced behavioral responses were analyzed to confirm the analgesic effect of radiation in our model. The differential expression of pain-related signals in the spinal cord was also analyzed using high-resolution 2-dimensional gel electrophoresis (2-DE) and mass spectrometry (MS). Validation of the radiation-induced analgesia-related proteins was attempted using Western blotting analysis and immunohistochemical staining.

The invasion of cancer cells in the ipsilateral hind paw was detected from 7 days and was evident from 14 days after the transplant. The difference in the behavioral responses due to the mechanical and cold thermal stimulation was sustained from day 7. The radiation-induced analgesia was evident 3 days and 7 days after the radiotherapy, with increased pain threshold to the mechanical stimulation in animals given radiotherapy. The pain threshold in response to the cold thermal stimulations was also decreased with radiation at day 14. It was thought that the analgesic effect of radiation was not related with tumor regression because the erosion and destruction of the

bone was not obviously reduced by radiation.

A reference 2-DE map of spinal cord protein of normal mice (group N) was shown. One hundred and nineteen spots were analyzed by mass spectrometry and the identities of 107 spots were established using MALDI-TOF mass spectrometry. More than 5-fold increased expression caused by tumor formation was reversed by radiation on tumor bearing mice in 12 proteins. Among these proteins, the proteins which were thought to be related in the process of pain signaling were secretagoin, syntenin, P2X purinoreceptor 6 (P2X6) and Ca²⁺/calmodulin-dependent protein kinase 1 (CaM kinase 1).

P2X6 is supposed to be involved in the ATP-mediated fast synaptic transmission. Syntenin may have a role at the pathways that control vesicular trafficking. The putative function of CaM kinase 1 is believed to be involved in mediating transcriptional activation of gene expression in response to changes in intracellular Ca²⁺ concentration. Secretagoin also involves the Ca²⁺-binding characteristics.

Western blotting analysis was attempted and the validation of protein was possible in P2X6. To examine the presynaptic neurotransmitter expression mediated by Ca²⁺-signaling cascade, the expression of calcitonin gene-related peptide (CGRP) and substance P was examined by immunohistochemical staining. The expression of CGRP which was increased by tumor formation was decreased by radiation.

It is thought that the down-regulations of the proteins identified in the current study are involved in the mechanism of radiation-induced analgesia. The approach used in the current study will provide valuable tools for further studies in this field.



Key words : radiotherapy, cancer, pain, nociceptor, proteomics

<본문>

Analysis of radiation-induced analgesia-related proteins
in an animal model of cancer pain

Hee Chul Park

Department of Medicine
The Graduate School, Yonsei University

(Directed by Professor Jinsil Seong)

I. INTRODUCTION

Metastasis to the bone is commonly detected in various malignant tumors.¹ Bone metastasis is associated with various symptoms such as devastating pain, skeletal fractures, difficulty in ambulation, neurologic deficits, and the overall low quality of life.² Breakthrough pain resulting from the bone metastasis is the most serious and highly debilitating symptom that is difficult to manage effectively.^{2,3} Radiotherapy is highly effective in relieving the pain due to bone metastasis. Radiation is one of the most effective treatment modality adopted to prevent the morbidity due to pathologic fracture and the spinal cord compression caused by bone metastasis.⁴ Radiation can relieve pain in 90% of patients regardless of tumor response to radiation.² Radiotherapy is effective even for patients with bone metastasis from hepatocellular carcinoma that is known to be relatively radio-resistant tumor.^{5,6}

It is speculated that radiation-induced analgesia is related to specific mechanisms other than tumor regression.⁵ Because radiotherapy is for the eradication of metastatic cancer cells, the reports describing the mechanism of radiation-induced analgesia are rare.^{2,7} To understand the precise mechanism

of analgesic effects mediated by radiation, it is needed to analyze multiple pain-related target signals, which is now possible through high throughput technology.⁸ It will provide more information about the specific features and mechanisms of the radiation-induced analgesia in the intervention of metastatic bone pain.

Here, to explore the mechanism of radiation-induced analgesia, we have developed the model of bone pain resulting from the invasion of cancer cells in C3H/HeJ mice. Using that animal model, the radiation-induced behavioral responses were analyzed to confirm the analgesic effect of radiation in our model. The differential expression of pain-related signals in the spinal cord was also analyzed using high-resolution 2-dimensional gel electrophoresis (2-DE) and mass spectrometry (MS).⁹ Validation of the radiation-induced analgesia-related proteins was attempted using Western blotting analysis and immunohistochemical staining.

II. MATERIALS AND METHODS

1. Animal model

C3H/HeJ mice, male, 8~10 weeks old were used. The animals were maintained at the specific-pathogen-free barrier of the Division of Laboratory Animal Medicine, Yonsei University College of Medicine. The temperature (22°C) and humidity (55%) were maintained. The water and diet were supplied *ad libitum*. The care and use of animals in this study were based on the Guidelines and Regulations for Use and Care of Animals at the Yonsei University.

A syngeneic hepatocellular carcinoma cells, HCa-1 derived from

C3H/HeJ mice, prepared in 5×10^5 cells in suspension were injected to periosteal membrane of hind foot dorsum, in the right side of the experimental animals. Animals were regularly examined for the tumor formation and their growth.

2. The detection of the invasion of cancer cells to the bone

Mice were sacrificed at the regular interval after the injection of tumor cells. Tumor-bearing hind paws were fixed in 4% zinc-buffered formalin in 0.1 M PBS at 4 °C overnight, decalcified in 10% EDTA (pH 7.4) for 2 weeks, and embedded in paraffin. Paraffin blocks were sectioned 7 μ m-thick, stained with Hematoxylin and Eosin, and examined under the light microscope.

3. The analysis of the behavioral responses to evoked pain stimulations

To monitor the development of pain resulting from the invasion of cancer cells to the bone, behavioral responses were measured at 1, 3, 5, 7, 14, 21, 28 days after the injection of tumor cells. In each group, 15 mice were used. Behavioral responses were analyzed by assessing the threshold of limb withdrawal or nocifensive behavior in response to the graded mechanical, radiant heat, or cold thermal stimuli. All the procedures were performed using a clear plastic observation chamber and mice were kept in the chamber at least 15 minutes, to habituate for experimental conditions.

The sensitivity to mechanical stimulation was determined by measuring the limb withdrawal threshold in response to the von Frey monofilament probing the plantar surface of ipsilateral hind paw. The withdrawal threshold was determined by assessing the 50% withdrawal in response to the stimulus (0.2, 0.4, 0.6, 0.8, 1, 2 mN of bending force) of 10

successive stimulations at the 10 seconds interval.

To assess the sensitivity to cold thermal stimuli, a drop of acetone (80%) was delivered to the plantar surface of ipsilateral hind paw. The experiments were repeated 5 times with 5 minutes interval and the withdrawal frequency was assessed.

Hyperalgesia to radiant heat was measured by the time-to-withdrawal (seconds) after application of the radiant heat stimulation with a halogen lamp. To prevent the injury from the radiant heat, the stimulation was discontinued if animals did not respond within 1 minute of the stimulation.

4. Radiotherapy

Radiotherapy was administered 15 days after the tumor transplant. Mice were immobilized in an acrylic jig and a single dose of 25Gy (1.5Gy/min) was delivered to the tumor-bearing area using 4 MV X-ray with linear accelerator. Radiation was given to tumor-bearing mice. So, the experimental animals divided into 3 groups including normal mice (group N), tumor-bearing mice (group T), tumor-bearing mice treated with radiation (group TR).

5. Two-dimensional SDS gel electrophoresis (2-DE) and image analysis

To determine the pain-related signals in the spinal cord, mice were sacrificed 7 days after radiotherapy. Spinal cord segments L1-L5 were removed and their tissues were suspended in sample buffer containing 40 mM Tris-HCl, 7 M urea, 2 M thiourea, 4% (w/v) CHAPS (Bio-Rad, Hercules, CA), 100 mM 1,4-dithioerythritol (DTT; Sigma, St. Louis, MO), 0.2% (v/v) Bio-Lytes (Bio-Rad) and endonuclease (Sigma). Suspensions were sonicated

for approximately 30 sec and centrifuged for 1 h at 100,000 g to remove DNA, RNA and any particulate materials. The supernatants contained the total spinal cord proteins solubilized in sample buffer. Protein concentrations in the supernatants were determined according to the manufacturer's guidelines, using the Bio-Rad assay system (Bio-Rad). All samples were stored at -70°C until use.

Two-dimensional gel electrophoresis was performed in a Bio-Rad Electrophoresis system.¹⁰ One milligram of total spinal cord protein was used for each electrophoresis. Aliquots of spinal cord proteins in sample buffer were applied to immobilized pH 3-10 nonlinear gradient (IPG) strips (Bio-Rad). The first dimensional isoelectric focusing (IEF) was performed at 100,000 Vh. After IEF, the strips were equilibrated in the equilibration buffer containing 6 M urea, 2.5% (w/v) sodium dodecyl sulfate (SDS), 2% (v/v) DTT, 5 mM tributylphosphine, 50 mM Tris-HCl (pH 6.8) and 20% (v/v) glycerol (Sigma) for 10 min. The second dimensions were analyzed on 9-18% linear gradient polyacrylamide gels using the Protean XL system (Bio-Rad) at 20C. Immediately after electrophoresis, the gels were fixed in 40% methanol and 5% phosphoric acid and stained with Coomassie blue G 250 (Bio-Rad) for 24 h.

The stained gels were scanned using a GS-800 calibrated densitometer (Bio-Rad). The digitized gel images were normalized and comparatively analyzed using the PDQUEST program (v6.2, Bio-Rad). The percentage of the volume of the spot representing a certain protein was determined in comparison with the protein present in the 2-dimensional gels.

6. Protein identification by matrix-assisted laser desorption ionization time-of-flight mass spectrometry (MALDI-TOF MS)

For mass spectrometry fingerprinting, protein spots were directly cut out of the gels and destained with 50% acetonitrile in 25 mM ammonium bicarbonate and dried in a speed vacuum concentrator (Savant, Pleasanton, CA). Dried gel pieces were reswollen with 50 mM ammonium bicarbonate (pH 8.0) containing 100 ng/L trypsin (Promega, Lyon, France) and incubated at 37°C for 17 h. Supernatant peptide mixtures were extracted with 50% acetonitrile in 5% trifluoroacetic acid (TFA) and dried in a speed vacuum concentrator. Peptide mixtures were then dissolved in 4 L of 50% acetonitrile and 0.1% TFA. Aliquots of 0.5 L were applied to a large disk and allowed to air-dry. The matrix was α -cyano-4-hydroxycinnamic acid (Sigma) in 50% acetonitrile containing 0.1% TFA. Spectra were obtained using a MALDI-TOF mass spectrometer (Micromass, Manchester, UK).

Protein database searching was performed with MS-Fit (<http://prospector.ucsf.edu/ucsfhtml4.0/msfit.htm>) using the average molecular weight of the monoisotopic peptide ions. Database search with MS-Fit was performed using the value of mammalian species. Mass tolerance was allowed within 50 ppm using internal calibration.

7. Western blot analysis

Mice were sacrificed 7 days after radiotherapy. Spinal cord tissues (L1-L5) were cut into small pieces, washed 3 times in ice-cold phosphate buffered saline (PBS; pH 7.4) and lysed in a buffer containing 2% SDS, 20% glycerol, 10 mg/mL phenylmethylsulfonyl fluoride (PMSF) (Sigma) and leupeptin (Sigma). Suspensions were sonicated for approximately 30 sec and centrifuged at 20,000 g for 30 min. Protein samples (10 g) were loaded onto each lane, size fractionated by polyacrylamide gel electrophoresis, and transferred to a nitrocellulose membrane (Bio-Rad) in a transfer buffer

consisting of 48 mM/L Tris base, 20% methanol, 0.04% SDS, and 30 mM/L glycine.

After incubation with a blocking buffer consisting of PBS containing 0.1% Tween-20 (PBST) and 5% skimmed milk (Amersham International, Little Chalfont, UK), the membranes were incubated for 2 h at room temperature (RT) with primary antibody in the appropriate dilution, as recommended by the supplier. Primary antibody included the antibody to P2X purinoreceptor 6 (P2X6) (polyclonal, goat antibody; Santa Cruz biotechnology, Santa Cruz, CA) which was commercially available. After washing in PBST, the membranes were incubated for 1 h at RT in either an anti-goat IgG antibody conjugate (Santa Cruz biotechnology), which released chemiluminescence in the presence of horseradish peroxidase. ECL Western blotting detection system (Amersham International) was applied for chemiluminescence detection. Detectable proteins were quantified by densitometer (Raytest, Straubenhardt, Germany).

8. Immunohistochemical staining

Mice were sacrificed 7 days after radiotherapy. And the spinal cord tissues (L1-L5) were fixed for 16 hours with perfusion fixative, and cryoprotected for 24 hours in 0.1 M PBS with 30% sucrose. Serial frozen spinal cord sections, 60- μm thick, were cut by sliding microtome, collected in PBS, and processed as free-floating sections. The sections were stained with the antibody to calcitonin gene-related peptide (CGRP) (Monosan, Uden, Netherlands) and substance P (Calbiochem, San Diego, CA). Antibodies were used at the dilution recommended by the manufacturer.

9. The statistical analysis

Student's t-test was used to compare the behavioral responses and Western blot results. The difference was considered statistically significant if the p-value was less than 0.05.

III. RESULTS

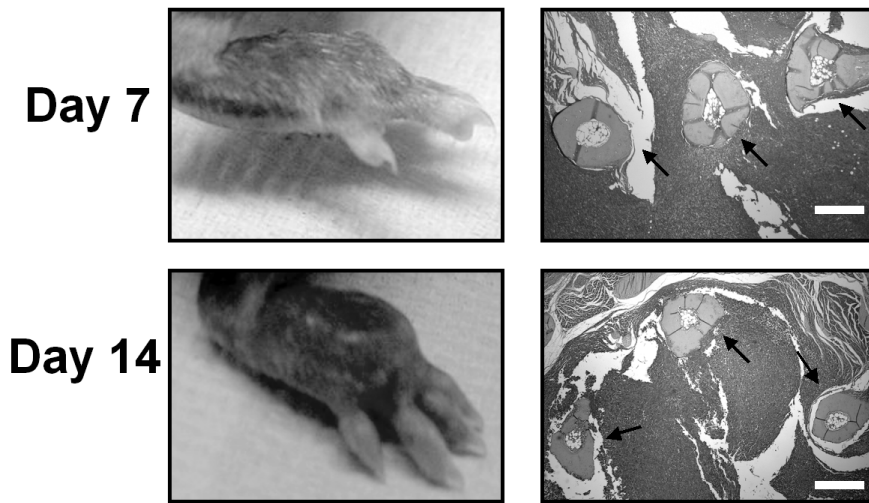
1. The establishment of an animal model

A. The detection of the invasion of cancer cells to the bone

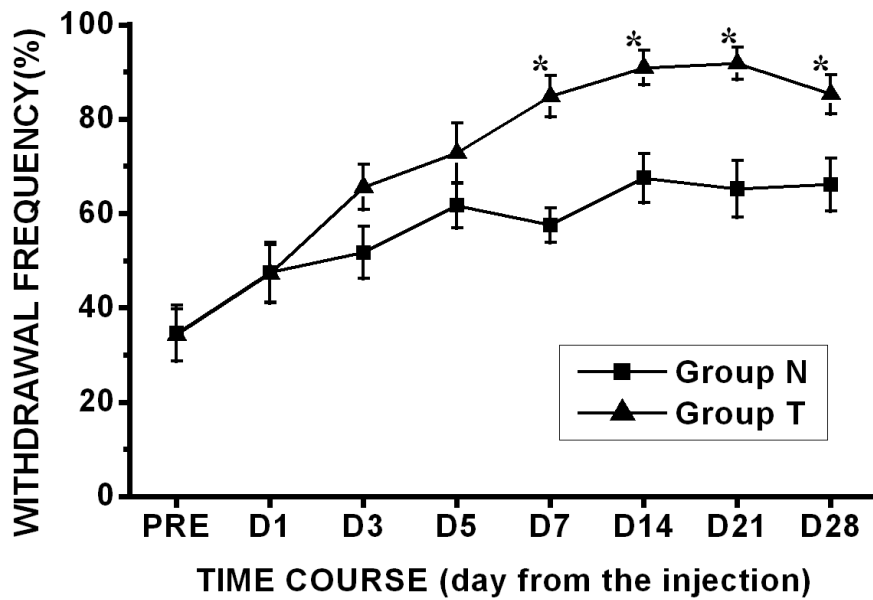
The invasion of cancer cells in the ipsilateral hind paw was detected from 7 days and was evident from 14 days after the transplant (Figure 1A). On the day 7, cancer cells attached to the periosteum of the metatarsal bones were detected. On the day 14, the obvious erosion and destruction of the metatarsal bone were detected.

B. Behavioral evidences of the development of bone pain resulting from the invasion of cancer cells to the bone

The pain in the bone due to the invasion of cancer cells was detected 7 days after injection (Figure 1B and C). The difference in the behavioral responses in response to the mechanical and cold thermal stimulation was sustained for both. From the day 7, the withdrawal frequency in response to the cold stimuli in animals bearing cancer cells was significantly higher than in control group (84.8 ± 4.4 vs. 57.5 ± 3.7 , $p < 0.05$). From the day 7, the threshold to the mechanical stimulation was also different in animals bearing tumors and control animals, 0.4 ± 0.03 vs. 0.6 ± 0.03 , respectively ($p < 0.05$).

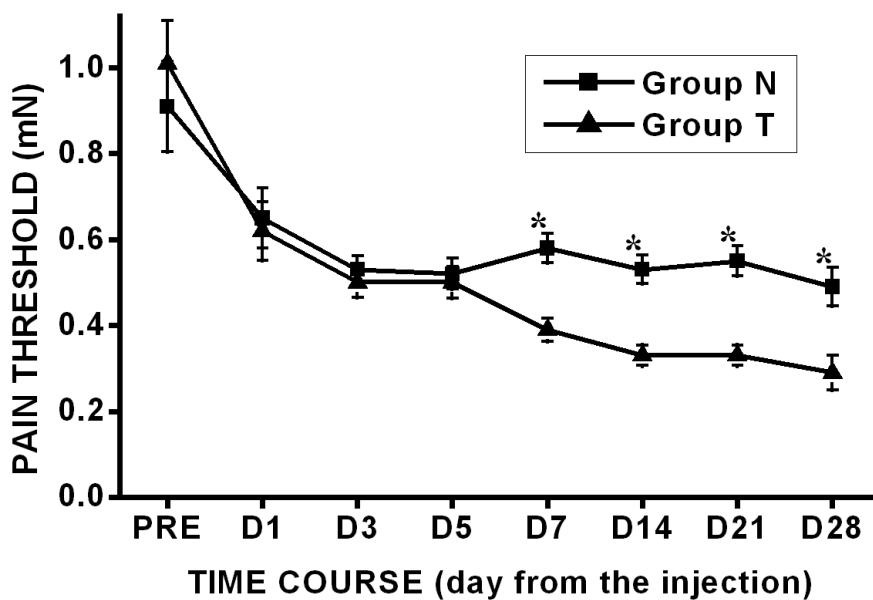


(A)



(B)

FIGURE 1. (continued)



(C)

FIGURE 1. The development of the hind paw model of bony pain due to invasion of cancer cells in the bone.

(A) Gross photos and histopathological examinations ($\times 40$, H & E staining) of ipsilateral hind paw, 7 and 14 days after injection of HCa-1 cells. Tumor formation was observed on the ipsilateral hind foot dorsum on the day 14. Cancer cells were attached to the periosteum of the metatarsal bones on the day 7 and the obvious erosion and destruction of the metatarsal bone were detected on the day 14 (see arrows). White scale bars: 500 μm .

(B) The result of acetone drop test. The withdrawal frequency in response to the cold thermal stimuli in animals bearing cancer cells (group T) was significantly higher than in control group (group N) from the day 7. *D_n* means *n* days from the injection of cancer cells. Asterisks(*) indicate that p-values are less than 0.05.

(C) The result of von Frey test. The threshold to the mechanical stimulation was different in animals bearing tumors (group T) and control animals (group N) on

the day 7. D_n means n days from the injection of cancer cells. Asterisks(*) indicate that p-values are less than 0.05.

However, the difference in the time to withdrawal due to the radiant heat was not detected (data not shown). Based on the data obtained from the histopathological analysis and the behavioral evidences, our experimental animals were considered having bone pain due to invasion of cancer cells in the bone.

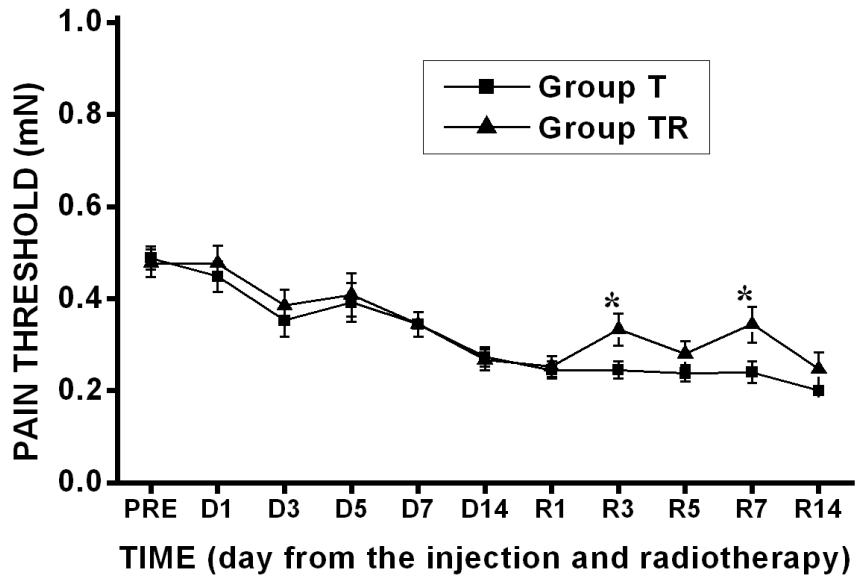
2. Radiation-induced relief of bone pain resulting from the invasion of cancer cells to the bone

To see whether radiation induces the analgesia in our models, the behavioral response to the mechanical and cold thermal stimulation was examined. The radiation-induced analgesia was evident 3 days and 7 days after the radiotherapy, with increased pain threshold to the mechanical stimulation in animals given radiotherapy (Figure 2A and B). The pain threshold in response to the cold thermal stimulations was also decreased with radiation. The difference in animals with and without radiation was statistically significant on the day 14 (Figure 2B). In the histopathological examinations, the obvious erosion and destruction of the metatarsal bone was not reduced by radiation (Figure 2C).

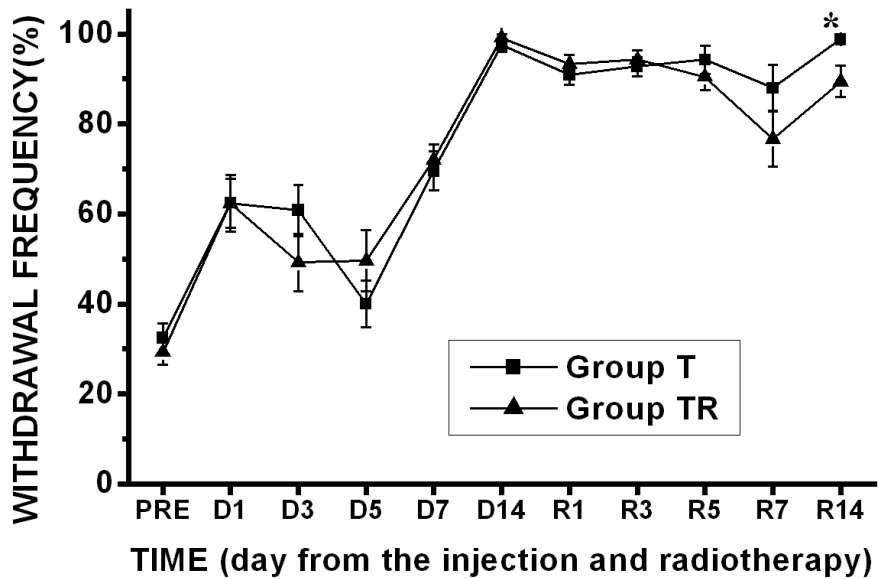
3. Two-dimensional SDS gel electrophoresis (2-DE) and matrix-assisted laser desorption ionization time-of-flight mass spectrometry (MALDI-TOF MS)

A. Proteins identified in the spinal cord

A proteomics approach was used to examine the differential expression of pain-related proteins in the spinal cord. Analyses were done for

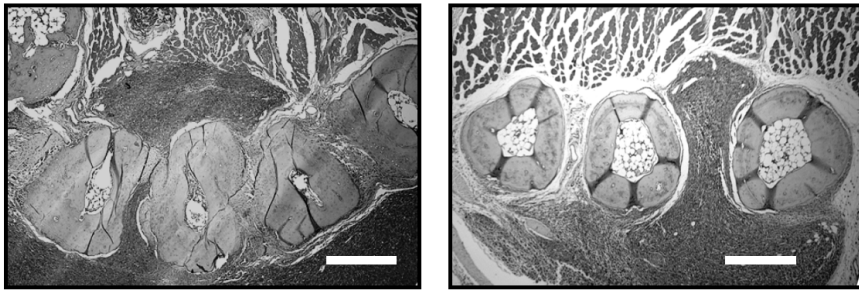


(A)



(B)

FIGURE 2. (continued)



Group T (R7)

Group TR (R7)

(C)

FIGURE 2. The relief of pain in the hind paw model of bony pain by radiotherapy.

(A) The result of von Frey test. The pain threshold to the mechanical stimulation in animals given radiotherapy (group TR) was increased on the day 3 and 7 after radiotherapy. Dn means n days from the injection of cancer cells, and Rn means n days from radiotherapy. Asterisks(*) indicate that p-values are less than 0.05.

(B) The result of acetone drop test. The pain threshold in response to cold thermal stimulations was also decreased with radiation (group TR) on the day 14. Dn means n days from the injection of cancer cells, and Rn means n days from radiotherapy. Asterisks(*) indicate that p-values are less than 0.05.

(C) Histopathological examinations ($\times 40$, H & E staining) of ipsilateral hind paw. R7 means 7 days from radiotherapy. The erosion and destruction of the metatarsal bone was not obviously reduced by radiation. White scale bars: 500 μm .

normal mice (group N), tumor-bearing mice (group T), tumor-bearing mice treated with radiation (group TR). The gels were obtained for spinal cord tissues of 5 mice for each group, respectively.

A reference 2-DE map of spinal cord protein of normal mice (group N) was shown (Figure 3). One hundred and nineteen spots were analyzed by mass spectrometry and the identities of 107 spots were established using MALDI-TOF mass spectrometry (Table 1). The remaining 12 spots were not identified, either because the peptide ions in the MALDI spectra were not sufficiently strong for unambiguous identification through MS-Fit or because the partial amino acid sequences did not match any translated nucleotide sequence in currently available databases.

B. The differential expression of protein in the spinal cord

The effects on the expression of spinal cord proteins by tumor formation in the ipsilateral hind paw and by radiation to the tumor-bearing area were summarized (Table 2). Tumor-bearing mice (group T) showed increased expression in 65 proteins and decreased expression in 7 proteins, respectively, compared to normal mice (group N). Tumor-bearing mice treated with radiation (group TR) showed increased expression in only 4 protein levels, and the level of expression in 81 proteins was decreased compared to tumor-bearing mice without radiation therapy (group T).

C. Radiation-induced analgesia-related proteins in the spinal cord

More than 5-fold increased expression caused by tumor formation was reversed by radiation on tumor-bearing mice in 12 proteins. These proteins are listed in Table 3. The proteins, their putative functions to be related in the

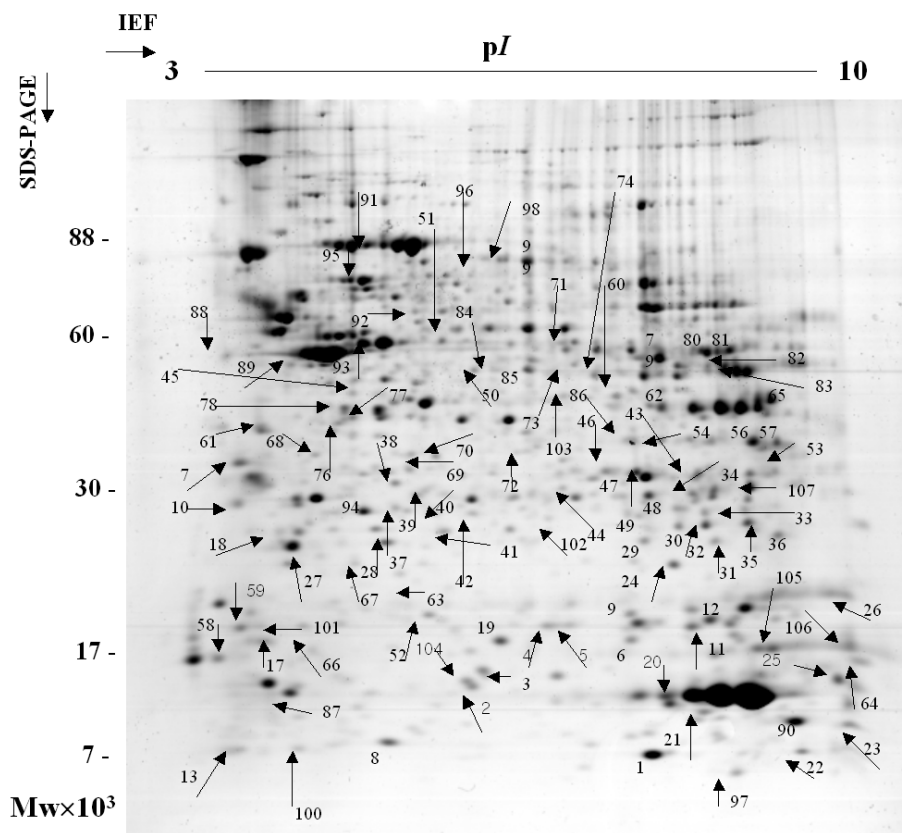


FIGURE 3. A reference 2-DE map of spinal cord protein of normal mice (group N). The first dimension is an isoelectric focusing immobilized pH gel ranging from pH 3 to pH 10 as indicated along the horizontal axis and the second dimension is a 9-18% SDS polyacrylamide gel where proteins are separated by their molecular weight, as indicated on the vertical axis. Proteins were stained and visualized by Coomassie brilliant blue G250. Arrows refers to spots that have been identified by mass spectrometry and the results are shown in Table 1.

Table 1. Proteins of mice spinal cord identified by MALDI-TOF mass spectrometry for the 2-D gel (pI 3.0 to 10.0) shown in Figure 1.

Spot	Acc. code ¹	Protein Identity	Function ²	Cov% ³	Mw/pI
1	4261685	Tyrosinase related gene	Signal ⁴	63	8416/7.3
2	22530892	methionine synthase	N metabolism ⁵	18	14628/6.1
3	Q05816	Fatty acid-binding protein	metabolism	55	15138/6.1
4	31417307	RPC155 protein	Signal	33	18272/6.5
5	14522868	Nervous system cytosolic sulfotransferase	N metabolism	29	19125/6.6
6	14495698	MPST protein	Signal	21	17382/7.1
7	13938440	Similar to protein phosphatase 1G	cell cycle	13	36636/4.2
8	Q29577	Creatine kinase	N metabolism	28	18606/5.3
9	35068	Nm23 protein	development	32	20412/7.1
10	18676452	FLJ00123 protein	miscellaneous	15	29690/4.3
11	13937981	Peptidylprolyl isomerase A	N metabolism	41	18012/7.7
12	10863927	Peptidylprolyl isomerase A	N metabolism	41	18013/7.7
13	Q9Y2B9	cAMP-dependent protein kinase inhibitor, gamma form	Signal	25	7911/4.1
14	4504351	Delta globin	miscellaneous	27	16056/7.8
15	P02593	calmodulin	Signal	23	17454/7.7
16	Q15304	Apoptosis regulatory protein Siva	Apoptosis	33	18695/7.9
17	Q9N1Q9	Calcium-binding protein CaBP2	Signal	43	18639/4.5
18	Q9UKA8	Calcipressin 3	Signal	17	27492/4.5
19	27807413	Prefoldin 5	Signal	24	17385/6.3
20	31745168	Resistin-like gamma; RELMgamma	miscellaneous	18	11783/7.4
21	P49458	Signal recognition particle 9kDa protein	Signal	30	10112/7.8
22	13492060	Truncated beta-globin	miscellaneous	45	6542/9.1
23	Q8WTQ1	Beta defensin 4	miscellaneous	45	8512/9.4
24	12838743	Unnamed protein	miscellaneous	20	23538/7.6
25	13430874	Hypothetical protein	miscellaneous	21	15054/9.4
26	37359860	mKIAA0242 protein	embryogenesis	22	21854/9.3
27	9055238	Voltage-gated sodium channel beta-3 subunit	Signal	30	24704/4.7
28	P31944	Caspase-14 precursor	Apoptosis	11	27680/5.4
29	21740307	Hypothetical protein	miscellaneous	32	24527/7.2
30	21669531	Immunoglobulin lambda light chain VLJ region	immune	22	27940/7.5

31	20380206	RAB39	Signal	33	25007/7.6
32	14250255	Fbxw1b protein	miscellaneous	14	28425/7.8
33	23110929	Proteasome beta 8 subunit isoform E2 proprotein	immune	23	30355/7.6
34	O08859	TNF inducible protein (TNF-stimulated gene 6 protein)	cytokine	12	30924/7.6
35	13619404	dJ782G3.1 (Liver-specific BHLH-ZIP transcription factor)	Signal	21	28042/8.1
36	5931741	Zinc finger protein	Signal	30	25878/8.4
37	31874028	Hypothetical protein	miscellaneous	30	29753/5.3
38	3757661	Secretagogin	Signal	21	32068/5.3
39	22003862	Retinal degeneration B beta	signal	22	31773/5.4
40	971538	MBq21	miscellaneous	26	28997/5.9
41	6014946	DEAD-box RNA helicase DEAD2	signal	15	27978/5.9
42	21669491	Immunoglobulin lambda light chain VLJ region	immune	14	28322/6.1
43	7523461	Serine/threonine protein phosphatase	signal	22	34345/7.7
44	7949150	Syndecan binding protein, syntenin	signal	14	32264/6.0
45	34680904	Riken c DNA	miscellaneous	21	49014/5.2
46	Q9JKF7	Mitochondrial 39s ribosomal protein L39	miscellaneous	15	34500/7.0
47	15530256	FLJ12571 protein	miscellaneous	21	31589/7.2
48	12847927	Unnamed protein	miscellaneous	10	31624/7.5
49	Q9HA64	Hypothetical fructosamine kinase-like protein	miscellaneous	19	34441/7.2
50	17932720	AIOLOS isoform 3	signal	40	53321/5.8
51	20988729	Pde2a protein	signal	23	58961/5.5
52	12805105	Snx12 protein	signal	24	19247/5.8
53	Q60660	Killer cell lectin like receptor 2	immune	21	33608/8.4
54	30578416	Zinc finger protein 183-like 1	signal	33	36259/7.5
55	P25388	Guanine nucleotide-binding protein beta subunit-like protein 12.3	signal	20	35077/7.6
56	P17431	Butyrate response factor 1	miscellaneous	18	36399/8.1
57	Q13829	TNF--induced protein 1, endothelial (B12 protein)	cytokine	18	36202/8.3
58	4885109	Calmodulin 3	signal	38	17163/4.1
59	15214615	Supt 16h protein	miscellaneous	12	21838/4.4
60	7435741	Proteasome endopeptidase complex	miscellaneous	21	44161/7.1

61	15080276	Similar to FGFR1 oncogene partner	signal	13	40922/4.5
62	Q9JKU8	LIM homeobox transcription factor 1 A	miscellaneous	13	42858/7.4
63	12654087	C2 or rF3 protein	signal	30	23627/5.2
64	21668858	Immunoglobulin heavy chain VHDJ region	immune	58	13397/9.6
65	O54803	P2X purinoreceptor 6	miscellaneous	16	42116/8.2
66	P04351	Interleukin-2 precursor	cytokine	31	19400/4.9
67	37653271	Heat shock factor Y protein	Stress protein	11	24272/5.1
68	2134950	Cyclic nucleotide gated channel gamma subunit	signal	21	32513/4.5
69	30704736	SNX27 protein	N metabolism	30	33256/5.4
70	15022614	Caspase-13B	Apoptosis	26	36925/6.1
71	O09039	Lymphocyte specific adapter protein Lnk	immune	12	60488/6.7
72	115576	Calpain 1	signal	26	35275/6.4
73	2773148	Msx-interacting zinc finger protein 1	signal	18	54052/6.7
74	P49410	Elongation factor Tu, mitochondrial precursor	signal	16	49399/6.7
75	Q9QZD9	Eukaryotic translation initiation factor 3 subunit 2	signal	19	36461/5.4
76	16758772	Cell growth regulatory with ring finger domain	signal	23	37443/5.1
77	23598135	MHC class I antigen	immune	16	39963/5.1
78	Q14012	Ca ²⁺ /calmodulin-dependent protein kinase type I	signal	33	41337/5.1
79	Q07130	UTP-glucose-1-phosphate uridylyltransferase 2	metabolism	20	55677/7.7
80	O08625	Synaptotagmin X	miscellaneous	11	57725/7.8
81	33469982	B lymphoid tyrosine kinase	immune	21	57707/8.0
82	P24549	Aldehyde dehydrogenase 1A	metabolism	20	54450/7.9
83	32822873	Was1 protein	signal	19	54259/8.0
84	P79386	Orphan nuclear receptor DAX-1	embryogenesis	22	52129/6.2
85	18256145	Fgd2 protein	signal	24	52531/6.4
86	24418885	Apoptosis-inducing factor(AIF)-homologous mitochondrion-associated inducer of death	apoptosis	26	36658/7.1
87	16923185	Immunoglobulin	immune	49	12843/4.7
88	33871444	NASP protein	embryogenesis	13	53739/4.3

89	809042	Laminin B1	N metabolism	29	54916/4.7
90	13385090	Cytochrome C oxidase	apoptosis	51	10072/9.0
91	32469766	Golgi autoantigen, golgin subfamily A member 1	signal	25	88201/5.2
92	P37173	TGF-beta receptor type II precursor	signal	15	64540/5.6
93	33859694	RIKEN cDNA 3110001H15	miscellaneous	11	60963/5.2
94	Q9Z2P6	Synaptosomal-associated protein 29	signal	30	29071/5.3
95	119531	Protein disulfide isomerase A4 precursor	stress protein	14	71974/5.1
96	7022159	Unnamed protein	miscellaneous	9	73605/6.1
97	8393250	Deleted in esophageal cancer 1	signal	14	7542/7.9
98	145480	Inhibitor of NFκB kinase, epsilon subunit	immune	11	80940/6.3
99	21359963	Constitutive photomorphogenic protein	DNA repair	13	80475/6.4
100	2429360	EWS/FLI1 activated transcript 2 homolog	signal	73	5043/4.6
101	25058850	SECP43 protein	signal	19	20403/4.4
102	5757900	Nitric oxide synthase	signal	23	30027/6.3
103	4504511	DNAJ homolog subfamily A member 1	Stress protein	16	44869/6.7
104	17981684	Cyclin-dependent kinase inhibitor	cell cycle	35	14722/6.1
105	1730504	Protegrin 2 precursor	miscellaneous	25	16478/8.1
106	14211923	PKCI-1-related HIT protein	signal	42	17162/9.2
107	Q60654	Killer cell lectin like receptor 7	cytokine	21	32522/8.1

¹ Acc. code means the accession code. The accession code refers to NCBI or SWISS-PROT database.

² The functions of the individual proteins were based on the current knowledge on molecular interaction networks, the KEGG pathway database at <http://www.genome.ad.jp/kegg/pathway.html>. If there were no available data, the description from the reference article in which the individual protein appears were utilized.

³ Percentage of coverage of full-length protein at 50 ppm for the MALDI-TOF peptides.

⁴ Signal means the function of individual proteins are involved in the pathway of signal transduction.

⁵ N metabolism mean the function of individual proteins are involved in the pathway of neuronal metabolism.

Table 2. The altered expression of spinal cord proteins by tumor formation in the ipsilateral hind paw of normal mice and by radiation to the tumor-bearing mice and normal mice.

Spot	Protein Identity	NT ¹	TTR ²	Function
2	methionine synthase	↑ 5	↓ 2	N metabolism
3	Fatty acid-binding protein	↑ 2	↓ 10	metabolism
4	RPC155 protein	↑ 2	↓ 5	Signal ³
5	Nervous system cytosolic sulfotransferase	↑ 2	↓ 5	N metabolism ⁴
6	MPST protein	↑ 5	↓ 2	signal
7	Similar to protein phosphatase 1G	↑ 10	-	cell cycle
8	Creatine kinase	↑ 2	↓ 2	N metabolism
9	Nm23 protein	-	↓ 2	development
10	FLJ00123 protein	↑ 10	↓ 2	miscellaneous
11	Peptidylprolyl isomerase A	↑ 2	-	N metabolism
12	Peptidylprolyl isomerase A	↑ 2	↓ 10	N metabolism
13	cAMP-dependent protein kinase inhibitor, gamma form	↓ 5	↑ 5	signal
14	Delta globin	↑ 5	-	miscellaneous
16	Apoptosis regulatory protein Siva	↑ 5	↓ 2	Apoptosis
18	Calcipressin 3	↑ 5	-	signal
19	Prefoldin 5	↑ 2	↓ 2	signal
20	Resistin-like gamma; RELMgamma	↑ 2	↓ 5	miscellaneous
21	Signal recognition particle 9kDa protein	↑ 2	↓ 5	signal
22	Truncated beta-globin	↑ 10	-	miscellaneous
23	Beta defensin 4	↑ 10	↓ 2	miscellaneous
24	Unnamed protein	-	↓ 2	miscellaneous
25	Hypothetical protein	↑ 10	↓ 2	miscellaneous
26	mKIAA0242 protein	↑ 10	-	embryogenesis
27	Voltage-gated sodium channel beta-3 subunit	↑ 2	↓ 2	signal
28	Caspase-14 precursor	↑ 2	↓ 10	Apoptosis
29	Hypothetical protein	↑ 5	↓ 2	miscellaneous
30	Immunoglobulin lambda light chain VLJ region	-	↓ 2	immune
31	RAB39	↑ 10	↓ 2	signal
32	Fbxw1b protein	↑ 2	↓ 2	miscellaneous
33	Proteasome beta 8 subunit isoform E2 proprotein	↑ 10	↓ 2	immune
34	TNF inducible protein (TNF-stimulated gene 6 protein)	↑ 5	↓ 2	cytokine

35	dJ782G3.1 (Liver-specific BHLH-ZIP transcription factor)	-	↓ 10	signal
36	Zinc finger protein	↑ 5	-	signal
37	Hypothetical protein	-	↓ 5	miscellaneous
38	Secretagogin	↑ 5	↓ 5	signal
39	Retinal degeneration B beta	-	↓ 10	signal
40	MBq21	↑ 2	↓ 10	miscellaneous
41	DEAD-box RNA helicase DEAD2	-	↓ 10	signal
42	Immunoglobulin lambda light chain VLJ region	↑ 5	↓ 2	immune
43	Serine/threonine protein phosphatase	↑ 2	↓ 2	signal
44	Syndecan binding protein, syntenin	↑ 10	↓ 10	signal
46	Mitochondrial 39s ribosomal protein L39	↑ 2	↓ 5	miscellaneous
47	FLJ12571 protein	↑ 10	↓ 2	miscellaneous
48	Unnamed protein	-	↓ 10	miscellaneous
49	Hypothetical fructosamine kinase-like protein	↑ 5	↓ 2	miscellaneous
50	AIOLOS isoform 3	↑ 2	-	signal
52	Snx12 protein	-	↓ 5	signal
53	Killer cell lectin like receptor 2	↑ 5	↓ 5	immune
54	Zinc finger protein 183-like 1	↑ 10	↓ 2	signal
55	Guanine nucleotide-binding protein beta subunit-like protein 12.3	↑ 10	↓ 2	signal
56	Butyrate response factor 1	-	↓ 5	miscellaneous
57	TNF--induced protein 1, endothelial (B12 protein)	-	↓ 5	cytokine
58	Calmodulin 3	↑ 2	↓ 10	signal
59	Supt 16h protein	↑ 2	↓ 5	miscellaneous
60	Proteasome endopeptidase complex	↑ 2	↓ 5	miscellaneous
63	C2 or rf3 protein	-	↓ 2	signal
64	Immunoglobulin heavy chain VH DJ region	-	↓ 5	immune
65	P2X purinoreceptor 6	↑ 10	↓ 10	miscellaneous
66	Interleukin-2 precursor	↑ 10	↓ 10	cytokine
67	Heat shock factor Y protein	↑ 2	↓ 5	stress protein
68	Cyclic nucleotide gated channel gamma subunit	↑ 5	↓ 2	signal
69	SNX27 protein	-	↓ 5	N metabolism
70	Caspase-13B	-	↓ 2	Apoptosis
71	Lymphocyte specific adapter protein Lnk	↑ 10	-	immune
72	Calpain 1	-	↓ 5	signal
73	Msx-interacting zinc finger protein 1	↑ 5	↓ 5	signal
74	Elongation factor Tu, mitochondrial precursor	↑ 5	↓ 2	signal

75	Eukaryotic translation initiation factor 3 subunit 2	↑ 2	↓ 10	signal
76	Cell growth regulatory with ring finger domain	↑ 5	↓ 5	signal
77	MHC class I antigen	-	↓ 10	immune
78	Ca ²⁺ /calmodulin-dependent protein kinase type I	↑ 5	↓ 10	signal
79	UTP-glucose-1-phosphate uridylyltransferase 2	-	↓ 10	metabolism
80	Synaptotagmin X	↑ 2	↓ 10	miscellaneous
81	B lymphoid tyrosine kinase	↑ 2	↓ 10	immune
82	Aldehyde dehydrogenase 1A	-	↓ 5	metabolism
83	Was1 protein	↑ 10	↓ 2	signal
84	Orphan nuclear receptor DAX-1	↑ 2	↓ 10	embryogenesis
85	Fgd2 protein	↑ 5	↓ 2	signal
86	Apoptosis-inducing factor (AIF)-homologous mitochondrion-associated inducer of death	-	↓ 5	apoptosis
87	Immunoglobulin	-	↓ 5	immune
88	NASP protein	-	↓ 10	embryogenesis
89	Laminin B1	-	↓ 2	N metabolism
90	Cytochrome C oxidase	-	↓ 5	apoptosis
91	Golgi autoantigen, golgin subfamily A member 1	-	↓ 5	signal
92	TGF-beta receptor type II precursor	↑ 10	↓ 5	signal
93	RIKEN cDNA 3110001H15	↑ 10	-	miscellaneous
94	Synaptosomal-associated protein 29	↓ 5	-	signal
95	Protein disulfide isomerase A4 precursor	↓ 10	↓ 2	stress protein
96	Unnamed protein	-	↓ 5	miscellaneous
97	Deleted in esophageal cancer 1	↓ 5	↑ 5	signal
98	Inhibitor of NFκB kinase, epsilon subunit	↑ 10	-	immune
99	Constitutive photomorphogenic protein	↑ 5	-	DNA repair
100	EWS/FLI1 activated transcript 2 homolog	↑ 2	↓ 2	signal
101	SECP43 protein	↓ 5	-	signal
102	Nitric oxide synthase	-	↓ 10	signal
103	DNAJ homolog subfamily A member 1	↑ 5	-	stress protein
104	Cyclin-dependent kinase inhibitor	↑ 2	↓ 2	cell cycle
105	Protegrin 2 precursor	↑ 10	↓ 5	miscellaneous
106	PKCI-1-related HIT protein	↓ 2	↑ 10	signal
107	Killer cell lectin like receptor 7	-	↑ 5	cytokine

¹ NT means from the group of normal mice (group N) to the group of tumor-bearing mice (group T). (continued)

² TTR means from the group of tumor-bearing mice (group T) to the group of tumor-bearing mice treated with radiation (group TR).

³ Signal means the function of individual proteins are involved in the pathway of signal transduction.

⁴ N metabolism mean the function of individual proteins are involved in the pathway of neuronal metabolism.

↑ means increased expression of protein.

↓ means decreased expression of protein.

Numbers in the table means the fold-change of expression of individual protein.

Table 3. The proteins in which the increased expression caused by tumor formation was reversed by radiation on tumor-bearing mice.

Spot	Protein Identity	NT ¹	TTR ²	Function	Cov% ³
13	cAMP-dependent protein kinase inhibitor, gamma form	↓ 5	↑ 5	signal ⁴	25
38	<i>Secretagogin</i>	↑ 5	↓ 5	signal	30
44	<i>Syndecan binding protein, syntenin</i>	↑ 10	↓ 10	signal	21
53	Killer cell lectin like receptor 2	↑ 5	↓ 5	immune	21
65	<i>P2X purinoreceptor 6</i>	↑ 10	↓ 10	miscellaneous	16
66	Interleukin-2 precursor	↑ 10	↓ 10	cytokine	31
73	Msx-interacting zinc finger protein 1	↑ 5	↓ 5	signal	18
76	Cell growth regulatory with ring finger domain	↑ 5	↓ 5	signal	23
78	<i>Ca²⁺/calmodulin-dependent protein kinase type I</i>	↑ 5	↓ 10	signal	33
92	TGF-beta receptor type II precursor	↑ 10	↓ 5	signal	15
97	Deleted in esophageal cancer 1	↓ 5	↑ 5	signal	14
105	Protegrin 2 precursor	↑ 10	↓ 5	miscellaneous	25

¹ NT means from the group of normal mice (group N) to the group of tumor-bearing mice (group T). Numbers means the fold-change of expression of individual protein.

² TTR means from the group of tumor-bearing mice (group T) to the group of tumor-bearing mice treated with radiation (group TR). Numbers means the fold-change of expression of individual protein.

³ Percentage of coverage of full-length protein at 50 ppm for the MALDI-TOF peptides.

⁴ Signal means the function of individual proteins are involved in the pathway of signal transduction.

⁵ The comparison of the expression level of each protein appears in Figure 4.

↑ means increased expression of protein.

↓ means decreased expression of protein.

process of pain signaling and radiation-induced analgesia, were thought to be secretagogin (spot 38), syntenin (spot 44), P2X6 (spot 65) and Ca²⁺/calmodulin-dependent protein kinase type 1 (CaM kinase 1) (spot 78). The patterns of expression of these 4 proteins were compared in a portion of the original 2-D gels (Figure 4). Peptide mass spectrums for identification of these 4 proteins were shown in Figure 5.

4. Validation of the proteins

A. Validation of P2X purinoreceptor 6 by Western blot analysis

Validation through Western blot analysis was attempted and was shown in Figure 6. The antibody was only available for P2X6. The bands for P2X6 were identified consistently. However, there was no obvious change in the level of P2X6 by tumor formation or by radiation treatment.

5. The effector neurotransmitter mediated by cytosolic Ca²⁺ and Ca²⁺/calmodulin-dependent protein kinase type 1

To examine the effector neurotransmitter expression mediated by cytosolic Ca²⁺ and CaM kinase 1, the expression of CGRP and substance P on the spinal cord sections was examined 7 days after radiation. The expression of CGRP which was increased by tumor formation in tumor bearing mice without radiation (group T) was decreased in tumor-bearing mice treated with radiation (group TR) (Figure 7).

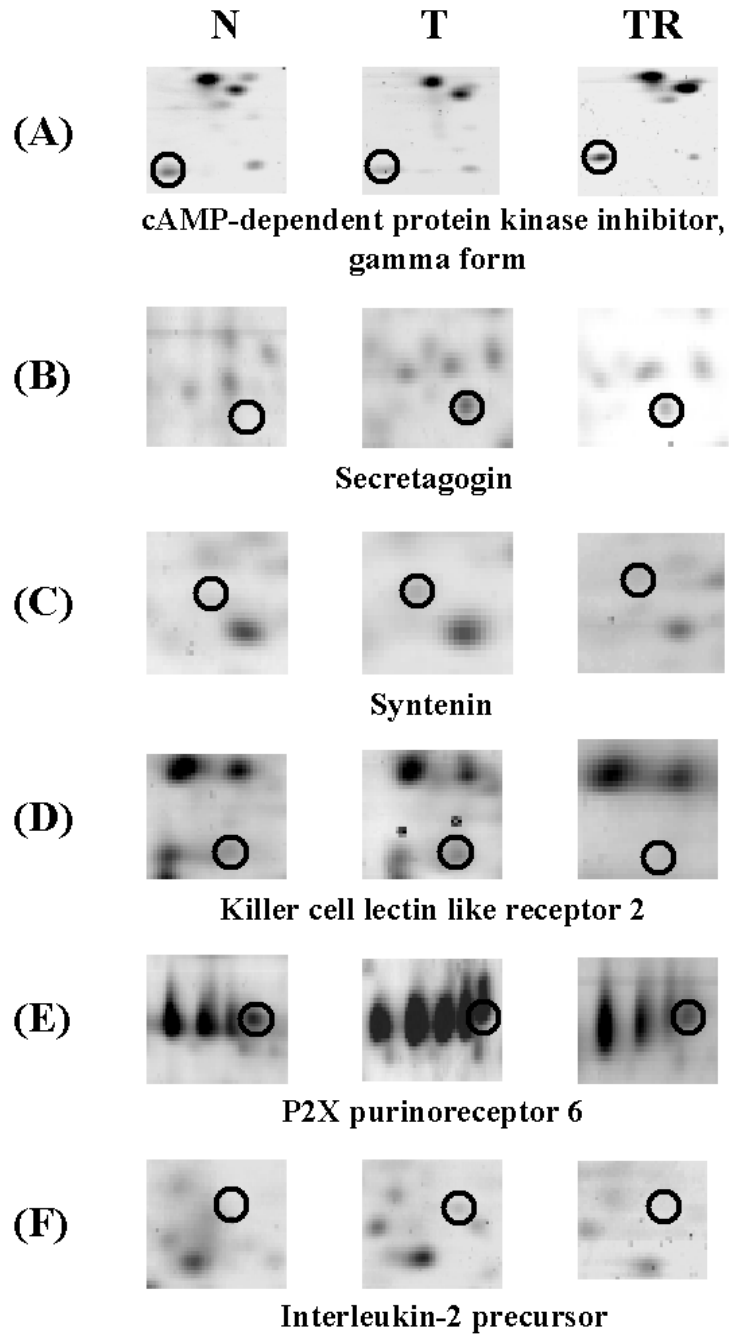


FIGURE 4. (continued)

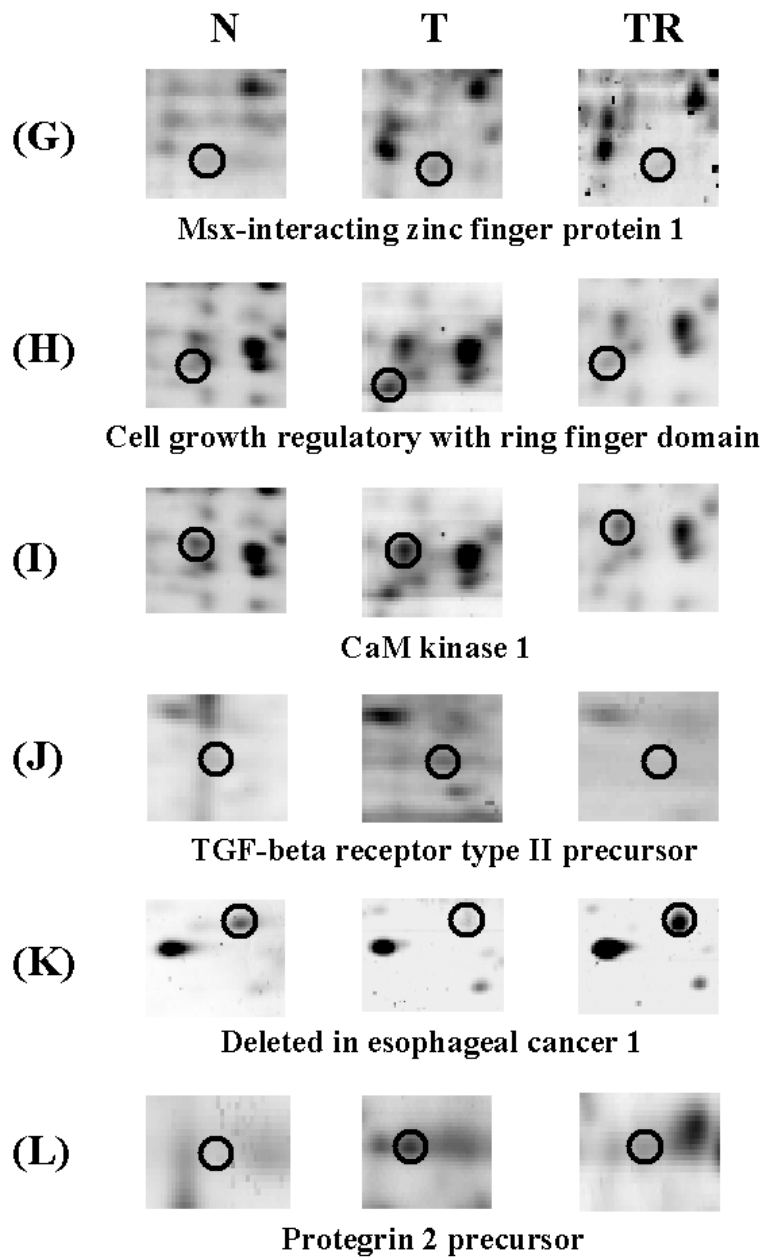


FIGURE 4. Coomassie brilliant blue G250 stained 2-D gels of spinal cord proteins of normal mice (N), tumor-bearing mice (T), and tumor-bearing mice (continued)

treated with radiation (TR), respectively. Each panel represents only a portion of the original gels, containing the protein showing significant increase in its expression by the formation of tumor and in which the expression level was reversed by the delivery of radiation on the tumor-bearing area.

- (A) The comparison of the expression of cAMP-dependent protein kinase, gamma form
- (B) The comparison of secretagogin expression
- (C) The comparison of syntenin expression
- (D) The comparison of the expression of killer cell lectin like receptor 2
- (E) The comparison of the expression level of P2X purinoreceptor 6
- (F) The comparison of the expression of Interleukin-2 precursor
- (G) The comparison of the expression of Msx-interacting zing finger protein 1
- (H) The expression of the expression of cell growth regulatory with ring finger domain
- (I) The comparison of the expression level of calcium/calmodulin-dependent protein kinase type 1.
- (J) The comparison of the expression of TGF-beta receptor type II precursor
- (K) The comparison of the expression of deleted in esophageal cancer 1
- (L) The comparison of the expression of protegrin 2 precursor

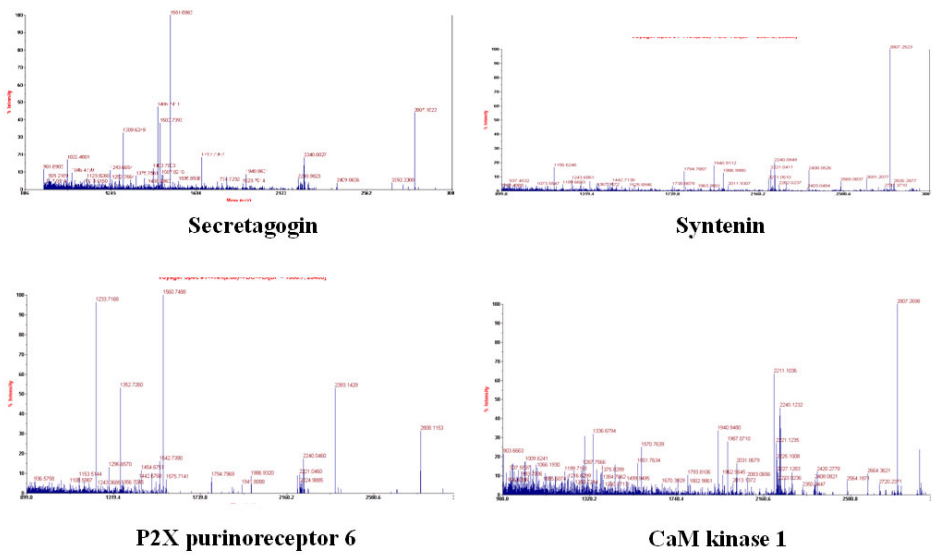


FIGURE 5. Identification of secretagoin, syntenin, P2X purinoreceptor 6 and CaM kinase 1 by MALDI-TOF mass spectrometry. Peptide mass spectrum was shown.

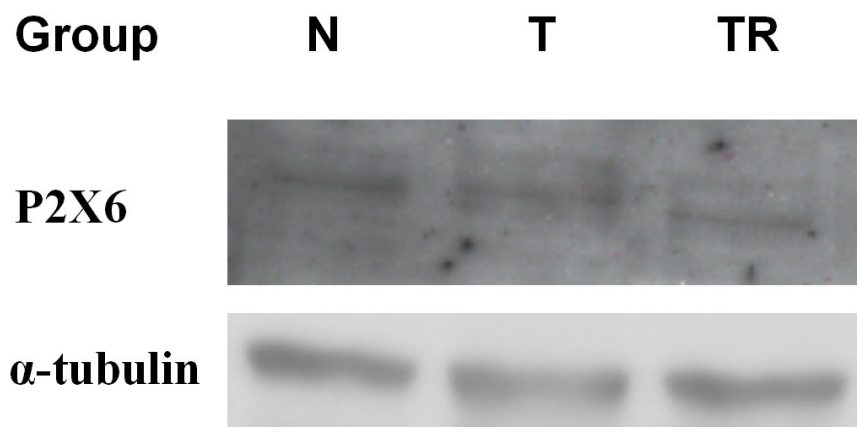


FIGURE 6. Western blot analysis of spinal cord proteins for P2X purinoreceptor 6 and α -tubulin in normal mice (N), tumor-bearing mice (T), and tumor-bearing mice treated with radiation (TR), respectively.

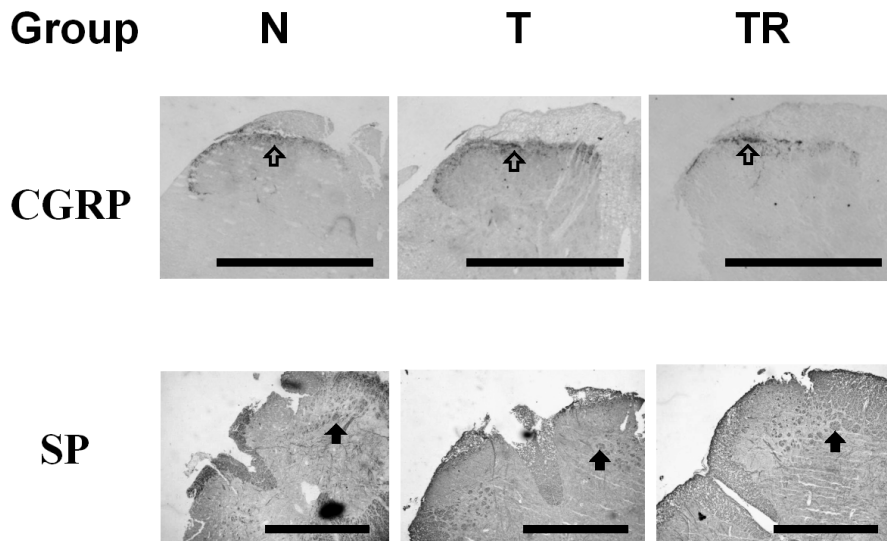


FIGURE 7. The changes of the pain-related signals in the spinal cord. The expression of calcitonin gene related peptide (CGRP) immunoreactivity was decreased in animals treated with radiation (group TR) comparing to that in untreated animals (group T) (see arrows). Scale bars: 500 μ m.

IV. DISCUSSION

Pain due to bone metastases may be nociceptive or neuropathic. The former is produced by stimulation of nociceptors in the endosteum by chemicals (derivatives of arachidonic acids such as prostaglandins and leukotrienes, substance P, bradykinin, histamine, IL-1, IL-6, and tumor necrosis factor-), stretching of the periosteum from increased tumor size, or micro-fracture.⁸ Neuropathic pain may be produced by the direct destruction of nerve tissue by tumors.¹¹ At times, both components are present. The stimulation of nociceptors leads not only to the propagation of pain sensation to the central nervous system but also winds up a vicious cycle resulting in hyperalgesia or allodynia.

Radiation can relieve pain in 90% of patients.² The mechanisms of pain relief after radiation therapy have not been defined clearly. Radiation-induced pain relief, which occurs later and is durable probably, is related to tumor cell kill. However, the pain relief with half-body irradiation is so rapid, as to be unlikely to be related to tumor cell kill.^{5,12} There are few reports concerning the mechanism of early relief of pain after radiotherapy.^{2,7} Hoskins et al.¹² suggested that radiotherapy intervened in the osteoclast activity. They reported that the reduction of bone resorption mediated by osteoclasts predicted the pain response in their observations.¹³ They also suggested that the analgesic effect by radiation is related to the inhibition of prostaglandin E2 produced by inflammatory cells in tumor tissue, without definite evidence.¹⁴ Goblirsch et al.¹⁵ reported in a recent publication that radiation treatment reduced bone pain and supported reduced cancer burden and reduced osteolysis as mechanisms through which radiation reduces bone cancer pain.

In the present study, we developed the animal model with bone pain due to invasion of cancer cells to the bone, which was confirmed by histopathological analysis and the pain-related behaviors (Figure 1). Using the animal model, we examined the radiation-induced relief of pain in the bone (Figure 2). We have observed that the radiation therapy relieved the pain in the bone as early as 3 days after radiation. At this stage of radiation induced analgesia, the obvious regression of tumor cell was not observed at all (Figure 2C). Actually, more than 80Gy of radiation is needed in controlling 50% of HCa-1 hepatocellular carcinoma cells, which is used for developing animal model in this study.¹⁶ This suggests that the radiotherapy-induced analgesia is mediated by the mechanisms different from the eradication of cancer cells.

Our data shows that radiotherapy attenuated the level of pain by altering the pain-related signals in the spinal cord (Table 3 and Figure 4, 5, 6). The proteins likely to be related in radiation-induced analgesia explored by proteomic analysis were secretagoin, syntenin, P2X6 and CaM kinase 1. The putative functions of the proteins explored, are thought to be involved in ATP-mediated fast synaptic transmission, Ca²⁺-signaling cascade and controlling vesicular trafficking. These proteins showed increased expression in its level by the invasion of cancer cells to the bone, and it was reversed by radiation therapy (Figure 4, 6).

Syntenin is strongly associated with membranes; localizes to cell-adhesion sites, microfilaments, and the nucleus; and physiologically interacts with syndecan-1. The versatile heparan sulfate moieties of syndecan-1 support various processes of molecular recognition, signaling, and trafficking.¹⁷ It is suggested that syntenin may have a role at the pathways that control vesicular trafficking, cytoskeletal dynamics, cell adhesion, and cell polarity.¹⁸ Beneyto et al.¹⁹ suggested that syntenin is involved in the process of anchoring glutamate receptor such as AMPA subunits to the cell membrane.

P2X purinoreceptors are a family of ligand-gated ion channels responsive to ATP.²⁰ Seven subtypes have been identified which form homomultimeric or heteromultimeric pores. P2X receptor activation of sensory neurons has been demonstrated in animal pain models, including the rat hind paw and knee joint preparations, as well as in inflammatory models.²¹ P2X4 and/or P2X6 receptors in the CNS also seem to be involved in pain pathways. Bardoni et al.²² suggested that ATP-activated P2X2, P2X4 and P2X6 receptors in laminae II of the rat spinal cord may play a role in transmitting or modulating nociceptive information. ATP-mediated synaptic transmission is likely to provide a new route for synaptically gated Ca²⁺ entry into dorsal horn neurons.

In many neurons, the depolarization leads to an increase in intracellular calcium, which can interact with calmodulin and modulate calcium-binding enzymes such as CaM kinases.²³ These effectors for intracellular Ca²⁺ as a second messenger molecules then mediate cellular responses by activating transcription factors that alter immediate early and delayed response gene expression. Of the five CaM kinases that have been identified, the expression level of CaM kinase 1 was changed by radiation in our study. The understanding on the function of CaM kinase 1 is relatively poor, than on which CaM kinases II and IV have been identified. Putative function of CaM kinase 1 is believed to be involved in mediating transcriptional activation of gene expression in response to changes in intracellular Ca²⁺ concentration.²⁴ Depolarization-mediated effects on CGRP induction are mediated via calcium and CaM kinase signal transduction pathway.²⁵ KN-62, which abolished the increase in CGRP caused by depolarization, blocks CaM kinase IV and V as well as CaM kinase II; a finding suggests that membrane depolarization acts via CaM kinase pathways to initiate CGRP expression.²⁶ Cytoplasmic Ca²⁺-binding proteins share a

unique tandem repeat of a Ca^{2+} -binding loop flanked by two helices known as the "EF-hand" Ca^{2+} -binding site. Secretagogen also shares these Ca^{2+} -binding characteristics.^{27,28} So, its putative function may involve the role in Ca^{2+} signaling cascade.

The trend of P2X6 expression in each experimental group explored by proteomic analysis was not reproduced by Western blotting analysis (Figure 6). The identification of P2X6 bands was consistent, however, there was no obvious change in the level of expression by tumor formation or by radiation treatment. Furthermore, more familiar neurochemical signatures, reported by other researchers, such as dynorphin, substance P, CGRP and etc, were not documented by proteomics in our study. Actually, the proteomic studies in neuroscience research have several shortcomings.²⁹ These are: (1) There are many low abundance proteins.(2) The important neurochemical targets are hydrophobic and are mainly represented by membrane proteins. So, the extraction of protein is difficult in some valuable candidate proteins. (3) High and low molecular weight proteins cannot be fairly separated. It will be rational to believe that the findings in the current study may missed some valuable proteins in explaining the mechanism of radiation-induced analgesia.

It is known that Ca^{2+} -related signaling cascade in the pre-synaptic primary afferent nerve fiber stimulates the release of excitatory amino acid (glutamate) and peptides like SP or CGRP. In the post-synaptic dorsal horn neurons, it stimulates the release of prostaglandin, NO, and NMDA receptor up-regulation. In the current study, radiotherapy decreased CGRP signals 7 days after radiation (Figure 7). CGRP is the primary afferent peptide with the strongest evidence of a role in pain perception. It is well known that the inflammations of peripheral tissues upregulates the production of CGRP in sensory ganglia, coincident with the development of hyperalgesia, and CGRP knockout mice have attenuated hyperalgesic responses.³⁰ It suggests that

radiation may mediate anti-inflammatory effects resulting in the relief of the pain.³¹ The anti-inflammatory effect of radiation has been reported and evidenced in various pathological conditions other than malignancy.³²

In case of metastatic bone pain, various sets of neurochemical changes occurs in the spinal cord according to the stage of metastatic evolution.⁸ The main mechanism can be inflammatory, mechanical or neuropathic. The mechanisms that generate and maintain pain status may be different among various cancer pain models.^{8,33} It will be also true that the reduction of CGRP signal in the spinal cord by radiation, which was shown in the current study, may not fully explain the mechanism of analgesic effect by radiation. The exact roles of the down-regulation of P2X6, secretagogen, CaM kinase 1 and synenin in the process of radiation-induced analgesia are still remained to be defined precisely. Though there was some discrepancy between the proteomic analysis and Western blotting analysis in P2X6, the down-regulations of these 4 proteins by radiation are relevant to the mechanism of radiation-induced analgesia.

The approach used in the current study will provide valuable tools for further studies in this field. It was thought that further studies should be directed to demonstrate the role of numerous candidate proteins, explored by proteomic analysis, involved in the mechanism of radiation-induced analgesia. It must be pursued how the radiation influenced the down-regulation of the proteins involved in radiation-induced analgesia in this study, especially in the scope of peripheral sensitization mechanism. And we performed this study in the resting status of experimental animal. It is needed to perform the studies exploring the radiation-induced analgesia-related proteins in the pain-evoked conditions.

V. CONCLUSION

We developed the animal model with bone pain due to invasion of cancer cells to the bone, which was confirmed by histopathological analysis and the pain-related behaviors. In this animal model, the radiation-induced analgesia was evident as early as 3 days after the radiotherapy. It was suggested that the radiotherapy-induced analgesia is mediated by the mechanisms different from tumor cell killing.

The differential expression of pain-related signals in the spinal cord was analyzed using high-resolution 2-dimensional gel electrophoresis (2-DE) and mass spectrometry (MS). The proteins, which were thought to be related in the process of pain signaling and radiation-induced analgesia, were secretagoin, syntenin, P2X6 and CaM kinase 1. Western blotting analysis was attempted and the validation of protein was possible in P2X6. The putative functions of the proteins explored by proteomic analysis, are thought to be involved in ATP-mediated fast synaptic transmission, Ca²⁺-signaling cascade and controlling vesicular trafficking.

The expression of CGRP which was increased by tumor formation was decreased by radiation in the analysis of immunohistochemical staining. It suggests that radiation may mediate anti-inflammatory effects resulting in the relief of the pain.

The approach used in the current study will provide valuable tools for further studies in this field. Further studies should be directed to demonstrate the role of numerous candidate proteins, explored by proteomic analysis, involved in the mechanism of radiation-induced analgesia.

REFERENCES

1. Nielsen OS, Munro AJ, Tannock IF. Bone metastasis: pathophysiology and management policy. *J Clin Oncol* 1991;9:509-524.
2. Mercadante S. Malignant bone pain: pathophysiology and treatment. *Pain* 1997;69:1-18.
3. Portenoy RK, Payne D, Jacobsen P. Breakthrough pain: characteristics and impact in patients with cancer pain. *Pain* 1999;81:129-134.
4. Powers WE, Ratanatharathorn V. Palliation of bone metastases. In: Perez CA, Brady LW, editors. *Principles and Practice of Radiation Oncology*. 3rd ed. Lippincott-Raven. 1998, p.2199-2217.
5. Koom WS, Seong J, Lee MJ, Park HC, Han KH, Chon JY, et al. Radiation therapy for bone metastasis from hepatocellular carcinoma. *Korean J Hepatol* 2002;8(3):304-311.
6. Kaizu T, Karasawa K, Tanaka Y, Matuda T, Kurosaki H, Tanaka S, et al. Radiotherapy for osseous metastases from hepatocellular carcinoma: a retrospective study of 57 patients. *Am J Gastroenterol* 1998;93(11):2167-2171.
7. Janjan NA. Radiation for bone metastases: Conventional techniques and the role of systemic radiopharmaceuticals. *Cancer* 1997;80(8):1628-1645.
8. Mantyh PW, Clohisy DR, Koltzenburg M, Hunt SP. Molecular mechanisms of cancer pain. *Nature Rev Cancer* 2002;2:201-209.

9. Lubec G, Krapfenbauer K, Fountoulakis M. Proteomics in brain research: potentials and limitations. *Prog Neurobiol* 2003;69:193-211.
10. Lim SO, Park SJ, Kim W, Park SG, Kim HJ, Kim YI, et al. Proteome analysis of Hepatocellular carcinoma. *Biochem Biophys Res Commun* 2002;291:1031-1037.
11. Ratanatharathorn V, Powers WE, Temple HT. Palliation of bone metastases. In: Perez CA, Brady LW, Halperin EC, Schmidt-Ullrich RK, editors. *Principles and practice of radiation oncology*. 4th ed. Philadelphia: Lippincott Williams and Wilkins; 2004. p.2385-2404.
12. Bates T, Yarnold JR, Blitzer P, Nelson OS, Rubin P, Maher J. Bone metastasis consensus statement. *Int J Radiat Oncol Biol Phys* 1992;23:215-216.
13. Hoskins PJ, Stratford MRL, Folkes LK, Regan J, Yarnold JR. Effect of local radiotherapy for bone pain on urinary markers of osteoclast activity. *Lancet* 2000;355:1428-1425.
14. Price P, Hoskins PJ, Easten D, Austin D, Palmer SG, Yarnold JR. Prospective randomized trial of single and multifraction radiotherapy schedules in the treatment of painful bone metastases. *Radiother Oncol* 1986;6:247-255.
15. Goblirsch M, Mathews W, Lynch C, Alaei P, Gerbi BJ, Mantyh PW, et al. Radiation treatment decreases bone cancer pain, osteolysis and tumor size. *Radiat Res* 2004;161:228-34.

16. Milas L, Wike J, Hunter NR, Volpe J, Basic I. Macrophage content of murine sarcomas and carcinomas: association with tumor growth parameters and tumor radiocurability. *Cancer Research* 1989;47:1069-75.
17. Grootjans JJ, Zimmermann P, Reekmans G, Smets A, Degeest G, Durr J, et al. Syntenin, a PDZ protein that binds syndecan cytoplasmic domains. *Proc Natl Acad Sci USA* 1997;94:13683-13688.
18. Zimmermann P, Tomatis D, Rosas M, Grootjans J, Leenaerts I, Degeest G, et al. Characterization of syntenin, a syndecan-binding PDZ protein, as a component of cell adhesion sites and microfilaments. *Molecular biology of the cell* 2001;13:339-350.
19. Beneyto M, Meador-Woodruff JH. Expression of transcripts encoding AMPA receptor subunits and associated postsynaptic proteins in the macaque brain. *J Comp Neurol* 2004;468(4):530-54.
20. Burnstock G. P2X receptors in sensory neurons. *Br J Anaesthesia* 2000;84(4):476-88.
21. Bland-Ward PA, Humphrey PPA. Acute nociception mediated by hindpaw P2X receptor activation in the rat. *Br J Pharmacol* 1997;122:365-71.
22. Bardoni R, Goldstein PA, Lee CJ, Gu JG, MacDermott AB. ATP P2X receptors mediate fast synaptic transmission in the dorsal horn of the rat spinal cord. *J Neuroscience* 1997;17(14):5297-304.
23. Means AR, Dedman JR. Calmodulin an intracellular calcium receptor.

Nature 1980;285;73-77.

24. Ghosh A, and Greenberg ME. Calcium signaling in neurons: molecular mechanisms and cellular consequences. Science 1995;268:239-247.

25. Ai X, MacPhedran SE and Hall AK. Depolarization stimulates initial calcitonin gene-related peptide expression by embryonic sensory neurons in vitro. J Neuroscience 1998;18(22):9294-9302.

26. Bito H, Deisseroth K, Tsien RW. Ca²⁺-dependent regulation in neuronal gene expression. Curr Opin Neurobiol 1997;7:419-429.

27. Wagner L, Oliyarnyk O, Garter W, Nowotny P, Groefer M, Kaserer K, et al. Cloning and expression of secretagoin, a novel neuroendocrine and pancreatic islet of langerhans-specific Ca²⁺-binding protein. J Biol Chem 2000;275(32):24740-24751.

28. Gartner W, Lang W, Leutmetzer F, Domanovits H, Waldhausl W, Wagner L. Cerebral expression and serum detectability of secretagoin, a recently cloned EF-hand Ca²⁺-binding protein. Cerebral Cortex 2001;11:1161-1169.

29. Lubec G, Krapfenbauer K, Fountoulakis M. Proteomics in brain research: potentials and limitations. Progress in Neurobiol 2003;69:193-211.

30. Hill RG. The role of CGRP in nociception? ScientificWorldJournal 2001;1(12 Suppl 1):19.

31. Hunt SP, Mantyh PW. The molecular dynamics of pain control. Nature Rev

Neurosci 2001;2:83-91.

32. Trott KR, Kamprad F. Radiobiological mechanisms of anti-inflammatory radiotherapy. *Radiother Oncol* 1999;51:197-203.

33. Honore P, Rogers SD, Schwei MJ, Salak-Johnson JL, Luger NM, Sabino MC, et al. Murine models of inflammatory, neuropathic and cancer pain each generates a unique set of neurochemical changes in the spinal cord and sensory neurons. *Neuroscience* 2000;98(3):585-598.

ABSTRACT(IN KOREAN)

암성 통증 동물 모델에서 방사선에 의한 통증 완화와 관련된
프로테오믹스 연구

<지도교수 성진실>

연세대학교 대학원 의학과

박 희 철

C3H/HeJ 웅성 마우스의 우측 발등에 암세포를 주입함으로써, 암세포의 침윤으로 뼈의 통증을 유발한 암성 통증 동물 모델을 수립하였다. 이 암성 통증 동물 모델을 이용하여 방사선에 의한 암성 통증의 완화 현상을 증명하고자 방사선 처치에 의해 유발되는 동물의 행동학적 변화를 관찰하고 분석하였다. 방사선에 의한 통증 완화의 기전을 파악하기 위하여, 종양의 형성과 방사선의 처치에 의해 변화하는 척수 부위의 통증 관련 단백질의 변화를 이차원전기영동과 단백질의 동정을 포함하는 프로테옴 분석 기법을 이용하여 분석하였다. 분석된 통증 관련 단백질을 확인하고자 Western blotting을 시도하였고 프로테옴 분석 기법을 이용하여 분석된 통증 관련 단백질의 2차적 신호전달을 통하여 발생하는 신경전달물질의 변화를 파악하기 위하여 면역조직화학염색을 시행하였다.

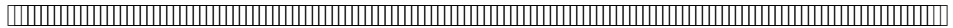
조직학적 관찰 결과 마우스의 발등에 암세포를 주입한 후 약 7-14일에 암세포의 뼈 침윤이 관찰되었고, 실험동물의 행동학적 변화를 통하여 시기적으로 암세포의 침윤과 암성 통증의 발생 시기가 일치함을 확인할 수 있었다. 방사선의 처치로 인한 암성 통증의 완화는 행동학적 변화의 관찰을 통하여 볼 때 약 3-7일 정도의 비교적 조기에 유도되었다. 그러나, 이 시기에 실험동물의 발등 부위에 발생한 암세포 침윤의 조직학적 변화는 없었다. 이를 통하여 방사선에 의한 암성 통증의 완화 현상은 암세포의 사멸과 직접적인 연관이 없음을 확인하였다.

프로테옴 분석 기법을 이용한 분석에서 107개의 척수 부위 단백질이 동정되었다. 종양의 형성 및 암세포의 침윤에 의하여 5배 이상 발현되는 수준이 변화하고, 이 후 방사선의 처치에 의하여 발현 수준의 변화가 반전된 단백질은 총 12개였다. 이 중 암성 통증 및 통증 전달 기작에 관여할 것으로 추정된 단백질은 4개로 secretagoin, syntenin, P2X purinoreceptor 6, Ca²⁺/calmodulin-dependent kinase 1 등이었다. 이들 단백질의 기능은 시냅스에

서의 신호전달의 가속, Ca²⁺의 신호전달, 세포내 vesicle의 교통정리 등에 관여하는 것으로 여러 연구자들은 보고하였다.

또한, 면역조직화학염색을 통하여 이 들 단백질의 2차적 신호전달을 통하여 CGRP의 발현 수준이 종양의 형성 혹은 암세포의 침윤에 의하여 증가하고 방사선 처치에 의하여 감소하는 것으로 관찰되었다. CGRP 혹은 substance P 등은 염증으로 인한 통증에 흔히 관여하는 신경전달물질로, 이는 간접적으로 방사선에 의한 통증 완화가 종양 혹은 암세포 침윤 부위에서 방사선에 의한 염증의 완화와 관련된 것으로 추정하였다.

본 연구에서 수립한 암성 통증 동물 모델은 향후 방사선에 의한 통증 완화와 관련된 여러 기전을 연구하는데 큰 역할을 할 수 있을 것이며, 향후 방사선에 의한 통증 완화에서 본 연구에서 분석된 통증 관련 단백질의 정확한 작용 기작을 규명하기 위한 더 많은 연구가 필요하다.



핵심되는 말 : 방사선치료, 암, 통증, 침해수용기, 프로테움